

Preparation and Thermoelectric Properties of $\text{Mg}_2\text{Si}_{1-x}\text{Ge}_x$ ($x=0.0 \sim 0.4$) Solid Solution Semiconductors[†]

Yasutoshi Noda*, Hiroyuki Kon*^{††}, Yoshitaka Furukawa*, Nobuyuki Otsuka*^{†††},
Isao A. Nishida** and Katashi Masumoto***

*Department of Materials Science, Faculty of Engineering, Tohoku University, Sendai 980, Japan

**National Research Institute for Metals, Tokyo 153, Japan

***Department of Electronic Materials, Faculty of Science and Technology, Ishinomaki Senshu University, Ishinomaki 986; Research Institute for Electric and Magnetic Materials, Sendai 982, Japan

$\text{Mg}_2\text{Si}_{1-x}\text{Ge}_x$ Solid Solution Semiconductors were prepared in the composition range $0.0 \leq x \leq 0.4$. At a composition $x=0.4$, effects of impurities were investigated for dopants of Sb and Ag. Carrier concentrations were controlled up to 1.5×10^{26} electrons/ m^3 and 5.5×10^{25} holes/ m^3 by doping Sb and Ag, respectively. The thermal conductivity κ was measured at 300 K. By calculating the electronic thermal conductivity κ_{el} based on the Fermi integration, the lattice thermal conductivity κ_{ph} was estimated to be $2.10 \text{ Wm}^{-1} \text{ K}^{-1}$. Figure-of-merits Z' 's of $\text{Mg}_2\text{Si}_{0.6}\text{Ge}_{0.4}$ at 300 K were $0.69 \times 10^{-3} \text{ K}^{-1}$ for the n-type sample with an electron concentration of $5.4 \times 10^{25} \text{ m}^{-3}$ (3000 ppmSb) and $0.47 \times 10^{-3} \text{ K}^{-1}$ for the p-type one with a hole concentration of $5.2 \times 10^{25} \text{ m}^{-3}$ (16000 ppmAg).

(Received March 24, 1992)

Keywords: dimagnesium silicon germanide, semiconducting solid solution, dopants, thermoelectricity, figure-of-merit, Fermi integral

I. Introduction

Mg_2X (X=Si, Ge and Sn) has an anti-fluorite-type structure (space group, Fm3m). The compounds were prepared in a graphite crucible⁽¹⁾⁻⁽⁵⁾ using a variety of reaction vessels such as iron⁽⁵⁾⁽⁶⁾, stainless⁽²⁾, quartz⁽³⁾, and graphite⁽⁴⁾. Then inert gas was introduced to minimize Mg loss by evaporation on the reaction, where the pressure was varied from 0.1 to 1 MPa⁽¹⁾⁻⁽⁵⁾⁽⁷⁾.

Mott and Jones pointed out that these compounds are semiconductors because the numbers of valence electrons are just equal to the number of states in Brillouin zones⁽⁸⁾. The energy gaps of Mg_2Si and Mg_2Ge were estimated to be 0.78 and 0.69 eV, respectively, from the temperature dependence of electrical conductivity in the intrinsic region⁽⁹⁾⁻⁽¹¹⁾. The semiconductive characteristics in the extrinsic region such as electrical conductivity, Hall coefficient, and thermoelectric power were reported in several literatures⁽¹⁾⁽¹²⁾⁻⁽¹⁴⁾. The thermal conductivities of Mg_2Si and Mg_2Ge up to 575 K were reported by LaBotz and Mason⁽²⁾. LaBotz *et al.*⁽¹⁵⁾ indicated that the solid-solution $\text{Mg}_2\text{Si}_{1-x}\text{Ge}_x$ is stable at the composition x from 0 to 1 and that the thermal conductivity reaches to the

minimum around $x=0.5$. The effect of the deviation from the stoichiometric composition was investigated in terms of the nominal excess content of Mg to the IV elements. Shunk⁽³⁾ showed that the deviation from the stoichiometric composition of Mg_2Ge causes the p-type conduction at the Mg-rich and n-type one at Mg deficient nominal compositions, while Mg_2Si is always the n-type independent of the Mg composition.

The doping elements such as Cu and Ag in Mg_2Si and Mg_2Ge act as acceptors⁽³⁾⁽¹²⁾⁽¹³⁾ and Sb in $\text{Mg}_2\text{Si}_{0.7}\text{Sn}_{0.3}$ as donors⁽⁷⁾. For the $\text{Mg}_2(\text{Si}, \text{Ge}, \text{Sn})$ solid solutions, the IB, IIB and IIIB group elements were predicted as acceptors, while the V, VI and VII ones as donors⁽¹⁶⁾. However it has not been confirmed experimentally.

The $\text{II}_2\text{-VI}$ solid solution for thermoelectric energy conversion was attractive material since the later-half of the 1970's when efficient utilization of energy became a significant matter of concern. Nicolaou⁽¹⁶⁾ reported the maximum efficiency of thermoelectric energy conversion of 37% for $\text{Mg}_2\text{Si}_x\text{Ge}_y\text{Sn}_{1-x-y}$ ($x=y=0.333$). The estimation was not obtained experimentally but deduced from the best data reported for the constituent binary and ternary compounds, although the details are unknown.

For the thermoelectric materials utilized for energy conversion, the optimum carrier concentration is recognized to be around 10^{25} m^{-3} . So far, fundamental studies of the thermoelectric properties, possible control of conduction type and carrier concentration have not been fully carried out for the $\text{II}_2\text{-IV}$ solid solution semiconductors.

In the present study, the n- and p-type samples of $\text{Mg}_2\text{Si}_{1-x}\text{Ge}_x$ were prepared by doping Sb and Ag, respec-

[†] This paper was originally published in Japanese in J. Japan Inst. Metals, 53 (1989), 487 and 55 (1991), 893.

^{††} Graduate Student, Tohoku University. Present address: Mitsui Mining and Smelting Co., Ltd., Ageo 362, Japan.

^{†††} Graduate Student, Tohoku University. Present address: Central Research Laboratory, Matsushita Electric Industrial Co., Ltd., Moriguchi 570, Japan.

tively, and their thermoelectric properties were investigated. The results indicate that they are promising materials with a high efficiency of thermoelectric energy conversion.

II. Experimental

The $\text{Mg}_2\text{Si}_{1-x}\text{Ge}_x$ samples were prepared by direct melting of constituent elements of Mg (nominal purity, 99.9%), Si (99.9999%) and Ge (99.9999%). Because of the deliquescence in the composition range $0.5 \leq x \leq 1.0$ ⁽¹⁵⁾, the sample composition studied was limited in the range $0 \leq x \leq 0.4$. Figure 1 shows a schematic diagram of the rf reaction furnace used. The crucible was made of graphite (0.1% ash, Tokai Carbon Ltd., No. G150). The dimensions of the crucible were 10 mm in dia. and 50 mm in length, and the bottom was shaped like a circular cone. The pressure inside the reaction furnace was 0.2 MPa of Ar (99.999%).

Prior to use, the crucible was heated at 1400 K in the stream of 0.1 MPa Ar in order to remove volatile impurities. The $\text{Mg}_2\text{Si}_{1-x}\text{Ge}_x$ solid solutions were synthesized at 1380 K which was about 20 K higher than the melting point of 1360 K⁽¹⁵⁾ at the composition $x=0.4$. The temperature gradient was about 10 K/cm from top to bottom of the crucible for the purpose of the uni-directional solidification. On cooling, the samples were kept at 1300 K for 3.3 h to homogenize the components and impurity elements and to proceed the grain growth.

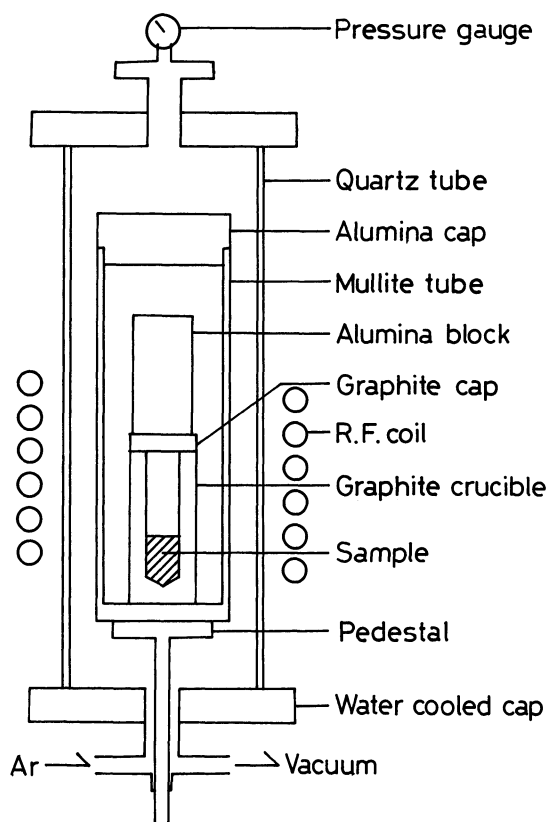


Fig. 1 Schematic diagram of the crystal growth apparatus.

The boiling point of Mg under 0.2 MPa Ar was estimated to be 1452 K using Clausius-Clapeyron's equation⁽¹⁷⁾⁽¹⁸⁾. The synthesis temperature was kept below the boiling point, which would be effective to suppress the evaporation of Mg. In order to avoid the reaction between the graphite crucible and the constituent elements, some samples were synthesized under the presence of NaCl, which had been adopted as a flux for the crystal growth of Si-compounds⁽¹⁹⁾.

The samples were analyzed by EPMA and identified by X-ray diffraction as a single phase of the anti-fluorite-type structure. The effect of dopants was investigated by using Sb (99.999%) and Fe (99.9%) for the n-type conduction, and Ag (99.9%), Cu (99.9%), B (99%), Al (99.9%) and In (99.999%) for the p-type one.

The thermoelectric power α was determined from the linear relationship between the thermoelectromotive force and temperature difference within 4 K. The resistivity and the Hall effect measurements were performed by the van der Pauw's method using the In-dotted contact. The thermal conductivity κ was measured for the undoped and Sb-doped samples applying the static comparison method at room temperature under the vacuum of 5×10^{-5} Pa and with a constant temperature difference within 2 K.

III. Results and Discussion

1. Undoped samples

As-grown boules were tapered at the bottom end and had dimensions of 10 mm dia. and 15 mm length. They were composed of coarse grains about 4 mm in diameter. Figure 2 shows the relationship between the composition analysed by EPMA and the lattice constant for the undoped samples. The relationship satisfies the Vegard's law and it is found that the difference between the nominal and analyzed compositions increases near $x=0.4$ probably due to the reaction between the elements and the crucible. However such a change in composition was scarcely observed for the samples grown by using the NaCl flux. From the X-ray diffraction investigation and

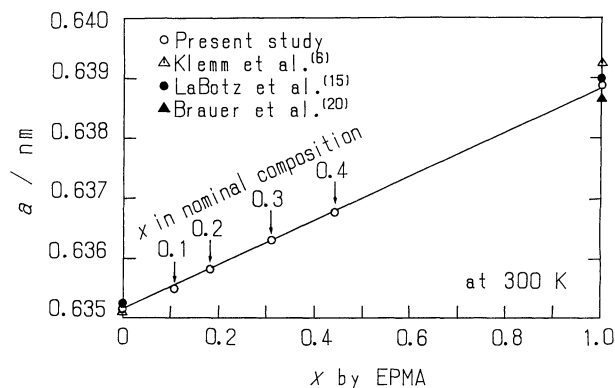


Fig. 2 Lattice constant as a function of the composition x of $\text{Mg}_2\text{Si}_{1-x}\text{Ge}_x$, determined by EPMA. Arrows indicate nominal compositions of samples grown without using NaCl flux.

the measured semiconducting properties, the as-grown boules were confirmed to be homogeneous. All the undoped samples of $\text{Mg}_2\text{Si}_{1-x}\text{Ge}_x$ were of the n-type and the thermoelectric power, the electrical conductivity σ and the electron concentration n were independent of the Ge content x . The composition of the samples were hereafter fixed at $x=0.40$, where κ takes a minimum and the samples are rather stable against moisture⁽¹⁵⁾.

2. Thermoelectric properties of $\text{Mg}_2\text{Si}_{0.6}\text{Ge}_{0.4}$

The samples used for measurements of the thermoelectric properties were cut from the middle part of the boules. Table 1 indicates the nominal and analyzed concentrations of the dopants, the conduction type and the carrier concentration of $\text{Mg}_2\text{Si}_{0.6}\text{Ge}_{0.4}$. It is shown that Sb acts as a donor and Cu or Ag as acceptors. In the case of Ag-doping, the analyzed concentration in the crystals was about 1/10 times the nominal one. Al and In have not been found to act as acceptors. B was first introduced as an acceptor by using the NaCl flux. Figure 3 shows the relationship between the doping amount of Sb and the carrier concentration. The electron concentration increased up to $1.5 \times 10^{26} \text{ m}^{-3}$. The broken line was derived by assuming that the Sb atom acts as a singly ionizable substitutional donor. When the doping level exceeds 10^3 ppm, the measured n differs from the calculated one. This deviation was ascribed to an increase in degeneracy, so that the Sb atom was not fully ionized.

The hole concentration is plotted in Fig. 4 against the nominal doping amount of B or Ag. A steep increase of p indicates that Ag incorporation into the host crystal lattice increases with increasing doping amount. The appearance of the maximum suggests that the carriers are compensated by the donors formed by Ag-interstitial atoms or complex. The broken line indicates the relationship between p and the nominal doping amount where each dopant atom can contribute a hole. The observed p values for the Ag-doped samples are lower than the calculated ones, while those for B doped samples are larger. The p increased up to $5.5 \times 10^{25} \text{ m}^{-3}$ and $2.0 \times 10^{26} \text{ m}^{-3}$ by Ag- and B-dopings, respectively. This result indicates that B-doping is suitable for controlling p over a wide range. However, homogeneous samples have

Table 1 Dopant and carrier concentration in $\text{Mg}_2\text{Si}_{0.6}\text{Ge}_{0.4}$ samples.

Dopant	Dopant concentration (ppm)		Type	Carrier concentration ($1/\text{m}^3$) at 300 K
	Nominal	Analyzed		
Sb	3200	3274	n	4.59×10^{25}
Sb*	3000	—	n	5.38×10^{25}
Fe*	6000	—	n	1.39×10^{25}
B	3200	—	n	1.34×10^{24}
B*	3500	—	p	1.02×10^{26}
Al	3200	<1200	n	1.49×10^{25}
Al*	6000	—	n	1.18×10^{25}
In	3200	<200	n	5.80×10^{24}
In*	6000	—	n	5.35×10^{24}
Cu	10000	566	p	4.50×10^{24}
Ag	40000	4230	p	3.50×10^{25}
Ag*	20000	—	p	4.45×10^{25}
Au	10000	<400	n	3.65×10^{26}

*Using NaCl flux on synthesis.

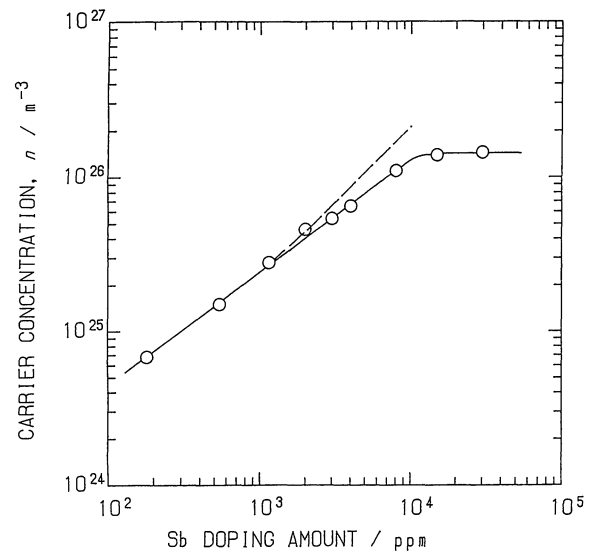


Fig. 3 Electron concentration as a function of Sb content at 300 K for $\text{Mg}_2\text{Si}_{0.6}\text{Ge}_{0.4}$ samples.

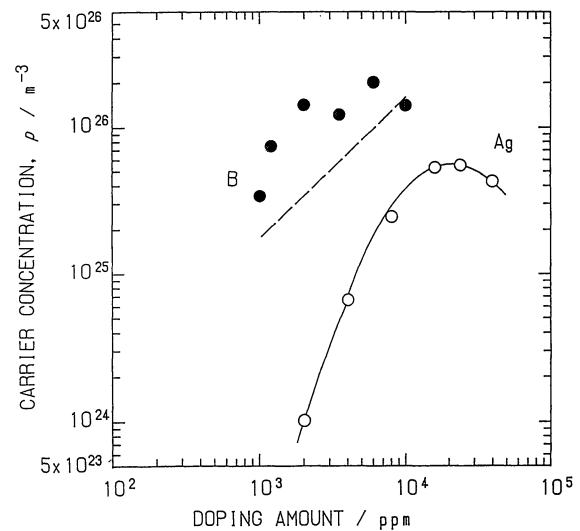


Fig. 4 Hole concentration as a function of dopant content at 300 K for $\text{Mg}_2\text{Si}_{0.6}\text{Ge}_{0.4}$ samples.

not been obtained because of the possible segregation of the B atom; the n-type was always observed at the bottom end of the boule. Figures 5 and 6 show α and σ as a function of carrier concentration at 300 K measured for the Sb- and Ag-doped samples, respectively. The α decreased and $\log \sigma$ increased monotonously with increasing $\log n$.

The observed thermal conductivities κ are listed in Table 2. The small value observed for the undoped sample is ascribed to the poor quality of the measured sample, indicating that the defects such as cracks are present in the boule. The κ is expressed by the sum of the components of phonon κ_{ph} and electron κ_{el} ⁽²¹⁾⁽²²⁾ as follows:

$$\kappa = \kappa_{\text{ph}} + \kappa_{\text{el}} \quad (1)$$

κ_{el} is expressed by the Wiedemann-Franz law, so that

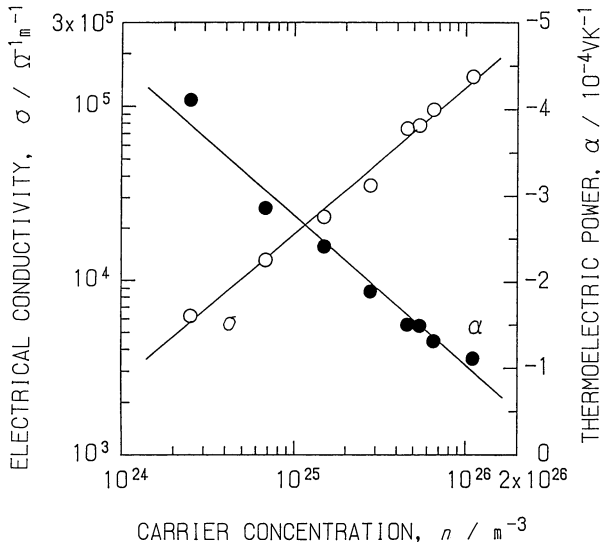


Fig. 5 Thermoelectric power and electrical conductivity at 300 K as a function of electron concentration for Sb-doped $\text{Mg}_2\text{Si}_{0.6}\text{Ge}_{0.4}$ samples.

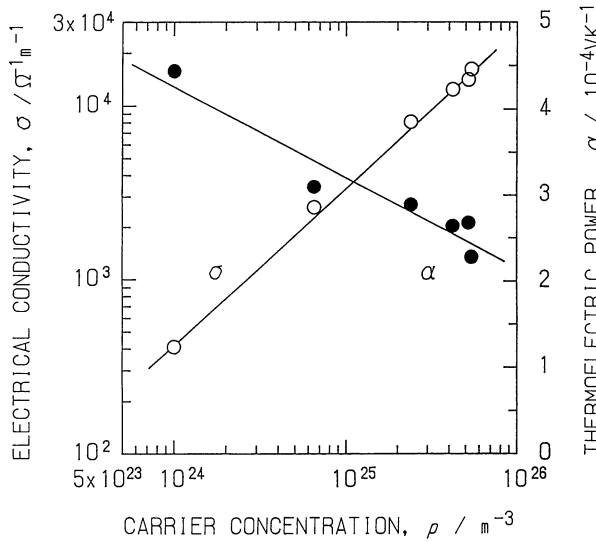


Fig. 6 Thermoelectric power and electrical conductivity at 300 K as a function of hole concentration for Ag-doped $\text{Mg}_2\text{Si}_{0.6}\text{Ge}_{0.4}$ samples.

$$\kappa_{\text{el}} = L \sigma T, \quad (2)$$

where L is the Lorentz number given by the expression

$$L = \frac{(k/e)^2 [(r+3)/(r+1)F_{r+2}(\xi)/F_r(\xi) - \{(r+2)/(r+1)F_{r+1}(\xi)/F_r(\xi)\}^2]}{2} \quad (3)$$

Here ξ is the reduced Fermi energy ($=\zeta/kT$, ζ : Fermi energy), k the Boltzmann constant, T the temperature, e the electron charge, and r the scattering factor which was determined to be 0.0 from the temperature dependence of the Hall mobility⁽²³⁾ corresponding to the acoustic phonon scattering⁽¹⁵⁾. $F_r(\xi)$ is the Fermi integral defined by

$$F_r(\xi) = \int_0^\infty \frac{x^r}{\{\exp(x-\xi) + 1\}} dx, \quad (4)$$

Table 2 Thermal conductivity and calculated values of electron and lattice thermal conductivities.

Sb amount (ppm)	κ (W/(m·K))	$\xi^{\#}$	$(10^{-8} L/V^2/K^2)$	κ_{el} (W/(m·K))	κ_{ph} (W/(m·K))
0	1.17	-2.512	1.499	1.07	1.60
1000	2.24	0.206	1.632	0.142	2.10
10000	2.50	2.457	1.917	0.410	2.09

[#]The system of $\xi < -2$ corresponds to a non-degenerated state, while $\xi > 2$ to heavily degenerated one (A. F. Ioffe: Semiconducting Thermoelements and Thermoelectric Cooling, Infosearch, London, (1958)).

and appears in the theoretical expression of the thermoelectric power⁽²⁴⁾:

$$\alpha = \pm (k/e) \{ (r+2)/(r+1) F_{r+1}(\xi)/F_r(\xi) - \xi \}, \quad (5)$$

where the positive and negative signs stand for the p- and n-type conduction, respectively.

ξ was estimated from the observed α values by eq. (5). Thus, κ_{el} was obtained by calculating L in eq. (3) using the measured σ -values. Table 2 indicates the ξ -, κ_{el} - and the resultant κ_{ph} -values. Since the κ_{ph} was nearly equal for the two Sb-doped samples, it is hereafter assumed that κ_{ph} is $2.10 \text{ W m}^{-1} \text{ K}^{-1}$ and independent of both the conduction type and the carrier concentration n . From the positive values of the reduced Fermi energy in Table 2, it is found that the Sb-doped samples are highly degenerated.

The κ values are calculated and plotted in Figs. 7 and 8 as a function of the carrier concentration for the n-type and p-type samples, respectively. By using the calculated thermal conductivity, the thermoelectric figure-of-merit,

$$Z = \alpha^2 \sigma / \kappa \quad (6)$$

was estimated as a function of carrier concentration and is shown in Figs. 9 and 10 for the n- and p-type, respectively. The maximum value of $Z_n(300 \text{ K}) = 0.69 \times 10^{-3} \text{ K}^{-1}$ was observed at $n = 5.4 \times 10^{25} \text{ m}^{-3}$ (nominal doping concentration: 3000 ppmSb) and $Z_p(300 \text{ K}) = 0.47 \times 10^{-3} \text{ K}^{-1}$ at $p = 5.2 \times 10^{25} \text{ m}^{-3}$ (16000 ppmAg).

The maximum figure-of-merit Z_{max} is expressed in terms of the semiconducting parameters⁽²⁵⁾:

$$Z_{\text{max}} \propto m^{*3/2} \mu T^{2/3} \exp(r+1/2) / \kappa_{\text{ph}}, \quad (7)$$

where μ is the carrier mobility. The values of these parameters are given in Table 3 for n- and p-type $\text{Mg}_2\text{Si}_{0.6}\text{Ge}_{0.4}$ at 300 K. The m^* was estimated from the relationship

$$n = 4\pi(2m^*kT)^{3/2} F_{1/2}(\xi) / h^3, \quad (8)$$

where h is the Plank constant. Table 3 also lists the values for lead telluride for comparison, which is the currently available material for efficient thermoelectric generators working between room temperature and 600–650 K. At room temperature, the Z_{max} -value of $\text{Mg}_2\text{Si}_{0.6}\text{Ge}_{0.4}$ remains lower than that of PbTe, which is ascribed to the low carrier mobilities. However, the low κ_{ph} and the heavy m^* in $\text{Mg}_2\text{Si}_{0.6}\text{Ge}_{0.4}$ are favorable factors

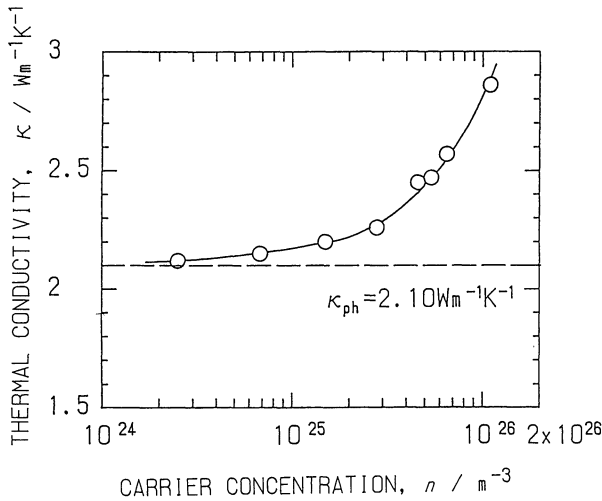


Fig. 7 Thermal conductivity of Sb-doped $\text{Mg}_2\text{Si}_{0.6}\text{Ge}_{0.4}$ samples as a function of electron concentration.

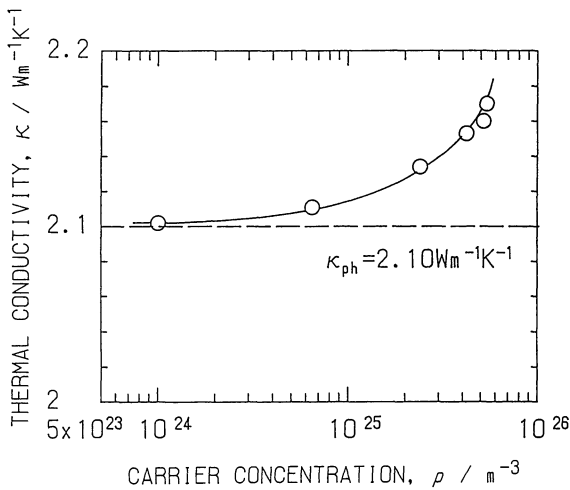


Fig. 8 Thermal conductivity of Ag-doped $\text{Mg}_2\text{Si}_{0.6}\text{Ge}_{0.4}$ samples as a function of hole concentration.

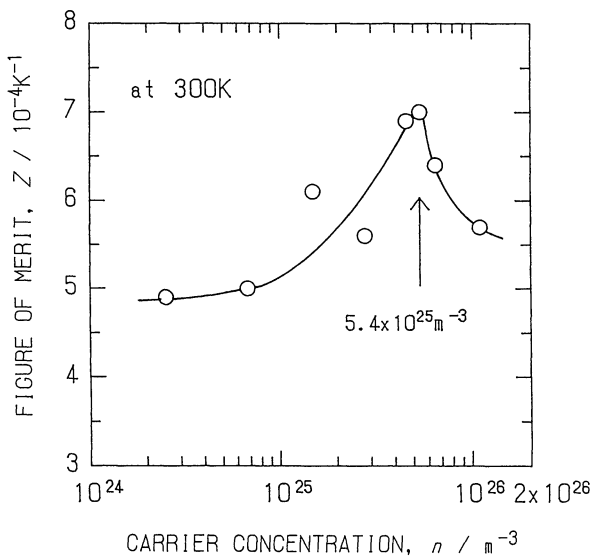


Fig. 9 Figure-of-merit versus electron concentration at 300 K for Sb-doped $\text{Mg}_2\text{Si}_{0.6}\text{Ge}_{0.4}$ samples.

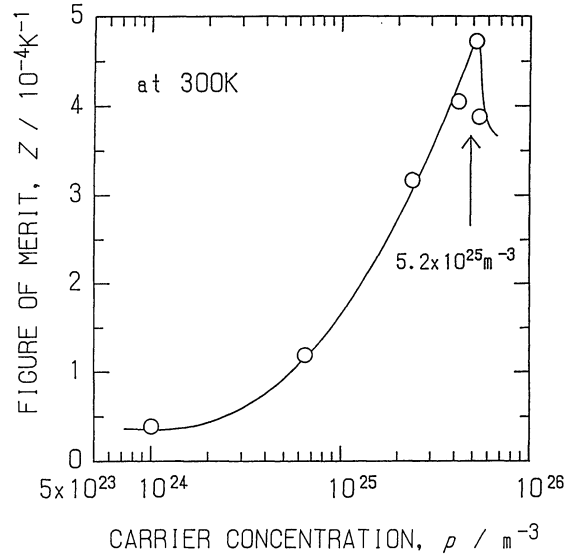


Fig. 10 Figure-of-merit versus hole concentration at 300 K for Ag-doped $\text{Mg}_2\text{Si}_{0.6}\text{Ge}_{0.4}$ samples.

Table 3 Semiconducting properties and figure-of-merit of $\text{Mg}_2\text{Si}_{0.6}\text{Ge}_{0.4}$ and PbTe.

	Type	m^*/m_0	μ ($10^{-4} \text{ m}^2 / (\text{V}\cdot\text{s})$)	κ_{ph} ($\text{W}\cdot\text{m} / \text{K}$)	μ/κ_{ph} ($10^{-2} \text{ m}\cdot\text{K} / (\text{W}\cdot\text{V}\cdot\text{s})$)	Z_{max} ($10^{-3} / \text{K}$)
$\text{Mg}_2\text{Si}_{0.6}\text{Ge}_{0.4}$	n	1.2 ± 0.2	108	2.10	0.51	0.69
	p	2.3 ± 1.2	22	2.10	0.10	0.47
PbTe [†]	n	0.13	1730	4.8	3.6	1.9
	p	0.15	840	4.8	1.8	1.2

[†]Data were taken from the Ref. (25).

which contribute to a higher value of Z . Further study must be done to attain a high carrier mobility and a high thermoelectric power, especially, by using the high-quality samples synthesized from the high-purity source elements.

IV. Summary

(1) Solid solution semiconductors $\text{Mg}_2\text{Si}_{1-x}\text{Ge}_x$ were prepared by the direct melting method. The reaction between the constituent elements and graphite crucible was suppressed by using the NaCl flux and the as-grown boules composed of coarse grains had almost the same composition as the nominal one.

(2) The carrier concentration in $\text{Mg}_2\text{Si}_{0.6}\text{Ge}_{0.4}$ were controlled by doping Sb as the donor and Ag as the acceptor. A significant result may allow us to apply this material to the thermoelectric generator.

(3) κ was measured at 300 K. By calculating κ_{cl} on the basis of the Fermi integration, κ_{ph} was estimated to be $2.10 \text{ Wm}^{-1} \text{ K}^{-1}$. From the semiconducting properties, Z_{max} 's were estimated to be $0.69 \times 10^{-3} \text{ K}^{-1}$ at $n = 5.4 \times 10^{25} \text{ m}^{-3}$ and $0.47 \times 10^{-3} \text{ K}^{-1}$ at $p = 5.2 \times 10^{25} \text{ m}^{-3}$.

(4) B-doping was made by using the NaCl flux, while

the other elements in group III had never been introduced as acceptors. It is to be noted that the B-doping indicates the possibility of controlling the hole concentration in a wider range than the group I(Ag) atom.

REFERENCES

- (1) R. G. Morris, R. D. Redin and G. C. Danielson: *Phys. Rev.*, **109** (1958), 1909.
- (2) R. J. LaBotz and D. R. Mason: *J. Electrochem. Soc.*, **110** (1963), 121.
- (3) H. R. Shanks: *J. Crystal Growth*, **23** (1974), 190.
- (4) E. N. Nikitin and V. K. Zaitsev: *Inorg. Mater.*, **2** (1966), 1698.
- (5) E. N. Nikitin, V. E. N. Tkalenko, V. K. Zaitsev, A. I. Zaslavskii and A. K. Kuznetsov: *Inorg. Mater.*, **4** (1968), 1656.
- (6) W. Klemm and H. Westlinning: *Z. Anorg. Allgem. Chem.*, **245** (1941), 365.
- (7) E. N. Nikitin, V. G. Bazanov and V. I. Tarasov: *Sov. Phys. Solid State*, **3** (1962), 2648.
- (8) N. F. Mott and H. Jones: *The Theory of the Properties of Metals and Alloys*, Clarendon Press, Oxford, (1963), p. 169.
- (9) G. Bush and U. Winkler: *Helv. Phys. Acta*, **26** (1953), 359.
- (10) G. Bush and U. Winkler: *Physica*, **20** (1954), 1067.
- (11) U. Winkler: *Helv. Phys. Acta*, **28** (1955), 633.
- (12) R. D. Redin, R. G. Morris and G. C. Danielson: *Phys. Rev.*, **109** (1958), 1916.
- (13) M. W. Heller and G. C. Danielson: *J. Phys. Chem. Solids*, **23** (1962), 601.
- (14) J. J. Martin: *J. Phys. Chem. Solids*, **33** (1972), 1139.
- (15) R. J. LaBotz, D. R. Mason and D. F. O'Kanne: *J. Electrochem. Soc.*, **110** (1963), 127.
- (16) N. C. Nicolau: *Proc. 1st Int. Conf. on Thermoelectric Energy Conversion (ICTEC)*, Arlington, (1976), p. 59; *Proc. 2nd ICTEC*, (1978), p. 82; *Proc. 3rd ICTEC*, (1980), p. 82; *Proc. 4th ICTEC*, (1982), p. 83; *Proc. 5th ICTEC*, (1984), p. 161.
- (17) J. M. Eldridge and K. L. Komarek: *Trans. Met. Soc. AIME*, **230** (1964), 226.
- (18) R. Hultgren, P. D. Desai, D. T. Hawkins, M. Gleiser, K. K. Kelley and D. D. Wagman: *Selected Values of the Thermodynamic Properties of the Elements*, American Society for Metals, Ohio, (1973), p. 294.
- (19) D. E. Elwell and H. J. Scheel: *Crystal Growth from High-Temperature Solutions*, Academic Press, New York, (1975), p. 31.
- (20) G. Brauer and J. Tiesler: *Z. Anorg. Allgem. Chem.*, **262** (1950), 319.
- (21) D. M. Rowe and C. M. Bhandari: *Modern Thermoelectrics*, Holt, Rinehart and Winston, London (1983), p. 18.
- (22) K. Uemura and I. Nishida: *Thermoelectric Semiconductors and their Applications*, Nikkan-Kogyo, Tokyo, (1988), p. 145.
- (23) Y. Noda, H. Kon, Y. Furukawa, I. A. Nishida and K. Masumoto: *Mater. Trans., JIM*, **33** (1992), .
- (24) I. J. Ohsugi, T. Kojima and I. Nishida: *J. Appl. Phys.*, **63** (1988), 5179.
- (25) Yu. I. Ravich, B. A. Efimova and I. A. Smirnov: *Semiconducting Lead Chalcogenides*, Plenum Press, New York, (1970), p. 323.